2024 European Control Conference (ECC)
June 25-28, 2024. Stockholm, Sweden

Online Data-driven Control of Networks

Karthik Shenoy[1], Ramkrishna Pasumarthy[1], Vijaysekhar Chellaboina[2]

Abstract— **Analysis and control of network systems largely rely on the availability of the network topology and the governing dynamics. In some cases, where the network dynamics and topology may not be available, researchers have relied on data-driven methods for the control of networks. A strict requirement of these methods is the collection of large amounts of persistently exciting data to enable control design. Moreover, these methods are largely restricted to linear systems and due to the open-loop nature of the control, lack robustness in the presence of external disturbances. In order to overcome these limitations, we present an online data-driven closed-loop control architecture for a nonlinear network system with unknown topology. Our method uses a novel 'cut-and-rewire' technique to assign a network topology that meets the desired control objectives while obviating the need for persistently exciting inputs and large open-loop offline data collection. We provide local asymptotic (exponential) stability guarantees for the closed-loop dynamics. We validate the results on a network of Kuramoto oscillators and achieve synchronization, phase balancing, and cluster formation when the underlying oscillator network topology is unknown and with noisy measurements.**

I. INTRODUCTION

A multitude of systems, both in nature and engineered, where more than one agent interacts with each other can be modeled as a set of dynamical equations coupled over a network. Some commonly found examples in nature include the synchronous behavior in the flashing of fireflies [1] and synchronizing behavior in heart pacemaker cells [2] to name a few. The control of complex networks has been a major area of research among the control community, which includes formation control of multi-agent systems [3], cluster synchronization [4], control of power-grid [5], analyzing controllability metrics of network systems [6], [7] and the propagation of opinions through social influencer networks [8]. In neurological systems the neural activity can be modeled as a network of Kuramoto oscillators [9] and certain neurological disorders like Parkinson's disease [10] and epileptic seizures [11] can be attributed to loss of synchronicity, and hypersynchrony of the neurons respectively. Deep brain simulations [12], which inject electrical impulses into specific sections of the brain to control the synchronization of multiple brain regions, are one of the most successful techniques for treating such illnesses. The control of complex networks is particularly challenging due to the high dimensionality of the state-space. In recent works on the geometric control of nonlinear dynamics on a network, the authors in [13] give conditions for feedback linearizability of network systems based on graph theoretic conditions, which reduces the computations required to check the feedback linearizability of large networks. Even though model-based control techniques provide tools to tackle problems in network control, they rely on the fact that the network topology is known. In general for a dynamical system, when the system dynamics are unknown, data-driven methods provide a means to design controllers directly based on system input-output or input-state data [14], [15], [16], [17], [18].

Related Work: In the case of data-driven control of networks, [19] provides a solution to the point-to-point control of states in open-loop for network systems using data, when the system dynamics and the network topology is unknown. The authors use offline input-output data to design optimal open-loop control signals to drive the node states from one point in state space to the desired point. However, the method requires a considerable amount of persistently exciting data points to be collected offline and is based on a linear approximation of the system. Moreover, since the method is open-loop, it is not robust to exogenous disturbances. Thus, to overcome these shortcomings, we propose a closed-loop feedback cancellation-based strategy for the control of networks with nonlinear node dynamics with unknown edges. The method does not require persistently exciting data sets as it is implemented online, and is novel with regard to the topology modification capability of the control architecture. The main contributions of this article are encapsulated below.

Contributions: We propose a novel two-part online data-driven control architecture for a nonlinear network unknown topology: The first part consists of an online data-driven estimator that estimates the states and the value of the nonlinear coupling terms at each instant without persistently exciting data samples. The second part is a feedback control law that utilizes a '*cut-and-re-wire*' strategy to assign a desired topology to the network. We provide Lyapunov-based guarantees for the asymptotic (exponential) stability of the desired equilibrium in closed-loop. We present a simulation-based validation for the control architecture proposed using a network of Kuramoto oscillators. We demonstrate that any desired behavior such as phase synchronization, phase balancing, and cluster formation can be achieved by assigning an appropriate topology. We demonstrate the robustness of the method, by introducing essentially bounded measurement noise into the system.

Notations and Preliminaries: $\text{col}\{x_1, \ldots, x_n\}$ represents the column vector with elements $\{x_1, \ldots, x_n\}$. $\mathbb{R}$, $\mathbb{R}^+$ represents the set of real numbers and the set of non-

[1]KS and RP are with the Dept. of Electrical Engineering, IIT-Madras, India. They are also associated with the Robert Bosch Center for Data Sciences and Artificial Intelligence at IIT Madras. {ee21d405@smail, ramkrishna@ee}.iitm.ac.in

[2] VC is the Dean of Engineering, GITAM (Deemed to be University), Visakhapatnam, India. dean_engineering@gitam.edu

negative real numbers respectively. $\mathbb{T}^n$ represents the n-torus or the cartesian product of n-circles. $\mathbf{1}_m$ corresponds to a column vector of ones, of length m. The big-O notation: $f(x,t) = O_x(T)$ implies $\exists\, K, T \in \mathbb{R}^+$ such that, $\forall t \in [0,T]$, $||f(t,x)|| \leq KT||x(t)||$. The estimate of a state $x(t)$ will be represented as $\hat{x}(t)$. The cardinality of a set X will be denoted as $|X|$. A graph $\mathscr{G} = (\mathscr{V}, \mathscr{E})$ is a collection of nodes $\mathscr{V} = \{1, 2, \ldots, n\}$, which could represent various subsystems in a dynamical system. Each subsystem can interact with one another via couplings or communication links, that are represented using edges $\mathscr{E} \subset \mathscr{V} \times \mathscr{V}$. The strength of coupling between each nodes can be represented by a scalar $w : \mathscr{E} \to \mathbb{R}$. The adjacency matrix of a graph is defined as $[A]_{ij} = w_{ij}$, if $(i, j) \in \mathscr{E}$ and 0 otherwise.

II. The Network Dynamics and Problem Formulation

Consider the dynamics of the i^{th} node, given by

$$\dot{x}_i = f_i(x) + b_i u_i \tag{1}$$

$$y_i = c_i x_i \tag{2}$$

where each $x_i \in \mathbb{R}$, such that $x = \text{col}\{x_1, \ldots, x_n\} \in \mathbb{R}^n$ is the state vector, $u_i \in \mathbb{R}$, $y_i \in \mathbb{R}$ are the input injected and the output respectively at the i^{th} node. b_i, c_i are the input and output gains respectively for the i^{th} node. The couplings or the interactions between nodes can be captured by a graph $\mathscr{G} = \{\mathscr{V}, \mathscr{E}\}$. Let $A \in \mathbb{R}^{n \times n}$ be the adjacency matrix for the graph. By convention, if there exists a directed edge from i^{th} to the j^{th} node, then $f_j(\cdot)$ is a function of x_i, i.e. the dynamics of the j^{th} node is influenced by the state x_i.

Various tools in literature, such as feedback linearization, provide a method to control the nonlinear network dynamics (1)-(2) provided we have complete knowledge of the edge set $\mathscr{E}$, and hence the coupling functions $f_i(\cdot)$. The lack of knowledge of how the subsystems interact with each other makes the problem challenging. Hence in this article, we pose the problem of designing control inputs u_i using data-driven techniques for a network of nonlinear dynamical systems (1)-(2) on a graph $\mathscr{G} = \{\mathscr{V}, \mathscr{E}\}$ such that the control law renders the $x^* \in \mathbb{R}^n$ locally asymptotically(exponentially) stable in feedback. The point x^* may belong to the span$\{\mathbf{1}_n\}$, in which case the states reach a consensus or synchrony. In other applications, the point x^* could refer to a particular formation of a collection of robots or cluster formation in coupled oscillator networks. Since the states, as well as the coupling functions $f_i(\cdot)$ are unknown, we need to estimate them in order to implement the feedback cancellation control law. We begin by designing a data-driven estimator in Section III. We define the feedback-cancellation-based 'cut-and-rewire' controller that assigns the desired topology to the network. We provide the main results that guarantee the asymptotic (exponential) stability of the point x^* in Section V. Finally, we validate the results on a network of Kuramoto oscillators in Section VII.

Remark 1. *The method proposed can be used to assign a desired topology to a selected subgraph $\mathscr{G}' = (\mathscr{P}, \mathscr{F})$ of $\mathscr{G}$ where $\mathscr{P} \subseteq \mathscr{V}$, $\mathscr{F} \subseteq \mathscr{E}$, $|\mathscr{P}| = p \leq n$, with the assumption that the network dynamics is minimum-phase (or the dynamics of the nodes $\mathscr{V} \setminus \mathscr{P}$ is stable). Henceforth, to broaden the scope of the study, we will focus on the control of nodes in a subgraph of a minimum-phase network system.*

III. Sampled-data system model and Data-driven Estimation

Due to the inherent discrete nature of data-driven controllers, we first discretize the dynamics (1), (2) for $i = 1, 2, \ldots, p \leq n$. We assume that the output is sampled using an ideal sampler and the input is injected via a zero-order hold. Let the sampling time be T. The sampled-data node dynamics, using Euler-Discretization is given by

$$x_i(k+1) = x_i(k) + T(f_i(x(k)) + u_i(k)) + O_x(T^2) \tag{3}$$

$$y_i(k) = x_i(k). \tag{4}$$

Now, for a small enough sampling time, the function $f_i(x(k))$ can be assumed to be constant in the interval $[kT, (k+1)T)$. Let $\sigma_i(k) := f_i(x(k))$ be the value of the function at the k^{th} instant. Taking $\sigma_i(k)$ to be an extended state, we can re-write (3) and (4) as

$$x_i(k+1) = x_i(k) + T(\sigma_i(k) + u_i(k)) + O_x(T^2) \tag{5}$$

$$\sigma_i(k+1) = \sigma_i(k) + O_x(T) \tag{6}$$

$$y_i(k) = x_i(k). \tag{7}$$

For a small enough sampling, neglecting the higher order terms in T, we can obtain a linear system model at each time instant, given by

$$\begin{bmatrix} x_i(k+1) \\ \sigma_i(k+1) \end{bmatrix} = E \begin{bmatrix} x_i(k) \\ \sigma_i(k) \end{bmatrix} + F u_i(k) \tag{8}$$

$$y_i(k) = H \begin{bmatrix} x_i(k) \\ \sigma_i(k) \end{bmatrix} \tag{9}$$

where $E = \begin{bmatrix} 1 & T \\ 0 & 1 \end{bmatrix}$, $F = \begin{bmatrix} T \\ 0 \end{bmatrix}$, $H = \begin{bmatrix} 1 & 0 \end{bmatrix}$. The estimate of the state $x_i(k)$ and the estimated state $\sigma_i(k)$ can be obtained using the estimator proposed in [18]. The data-driven estimator for (8), (9) is given by

$$\begin{bmatrix} \hat{x}_i(k) \\ \hat{\sigma}_i(k) \end{bmatrix} = (\mathscr{O}^T \mathscr{O})^{-1} \mathscr{O} [Y_i(k) + M U_i(k-1)] \tag{10}$$

where $\mathscr{O}$ is the 2×2 observability matrix of the pair (E^{-1}, G), $Y_i(k) = \text{col}\{y_i(k), y_i(k-1)\}$, $U_i(k-1) = \text{col}\{0, u_i(k-1)\}$, M is the matrix constructed using the of Markov parameters of (E^{-1}, F, G). The error in reconstruction can be shown to be of $O(T)$, Refer [18].

IV. Feedback Cancellation and topology re-assignment

The main objective of the controller is to cancel the nonlinear couplings present in the node dynamics and re-assign the network topology to achieve the desired behavior in the states of the nodes in the subgraph $\mathscr{P}$. Let the desired configuration of the states be denoted by $x^* \in \mathbb{R}^p$. We assume the following

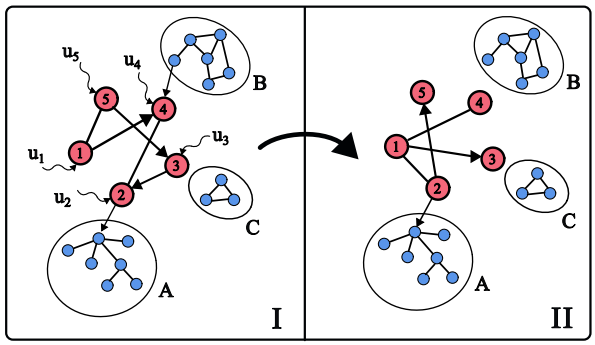

Fig. 1. In Figure I: an n-node graph with $p = 5$, and an unknown topology. The control inputs assign the desired topology to the subgraph shown in red, after cancelling the existing topology. In figure II, it can be seen that the incoming edges from subgraph B are canceled, whereas the edges that are outgoing to subgraph A are still present. Subgraph C is unaffected by the control inputs as it is not connected to any of the 5 nodes.

Assumption 1. *There exists a set of vector fields* $\text{col}\{g_1(\cdot), \ldots, g_i(\cdot)\}$, $i \in \mathscr{P} \subseteq \mathscr{V}$ *such that* $g_i(x^*) \equiv 0 \; \forall \, i \in \mathscr{P}$, $g_i(x + O_x(T)) = g_i(x) + O_x(T)$ *and, the point* x^* *is locally asymptotically (exponentially) stable with a region of attraction* $\mathscr{D}$*, such that* $x^* \in \mathscr{D} \subseteq \mathbb{R}^p$.

Once the estimate of the states, as well as the nonlinear couplings $f_i(\cdot)$ are obtained, the following control law (similar to feedback linearization) can be used to cancel the existing unknown nonlinear coupling and inject the desired dynamics $g_i(\cdot)$ into the nodes of the subgraph $\mathscr{P}$.

$$u_i(k) = -\hat{\sigma}_i(k) + g_i(\hat{x}(k)) \tag{11}$$

Remark 2. *The control law* (11) *will only cancel the effects of the incoming edges at the* i^{th} *node. The outgoing edges remain unaffected by the control law, as shown in Fig. 1.*

V. Main Results

In this section, we present the main results of the article which guarantees the asymptotic (exponential) stability of the desired equilibrium point, using the data-driven estimator designed in III and the control law given in Section IV.

Theorem 1. *Consider the node dynamics* (1)-(2)*, which is assumed to be minimum-phase, on a graph* $\mathscr{G} = (\mathscr{V}, \mathscr{E})$*, where the set of nodes* $\mathscr{V}$ *is known and the edges in* $\mathscr{E}$ *are unknown. Let Assumption 1 hold, such that the desired coupling functions be* $g_i(\cdot)$, $i \in \mathscr{P} \subseteq \mathscr{V}$*. Then the control law* (11)*, together with a data-driven estimator* (10)*, guarantee the existence of a sampling time* T^* *such that, for all* $T \in (0, T^*]$*, the states* $x \in \mathbb{R}^p$ *evolve along the flow given by the vector field* $\text{col}\{g_1(x), \ldots, g_p(x)\}$*. Furthermore, all trajectories starting in* $\mathscr{D}$ *converge to the state* $x^* \in \mathscr{D}$ *asymptotically (exponentially).*

Proof: The control law can only be executed after $k = 2$, as the data-driven estimator requires at least two data points to estimate the states as well as the coupling nonlinearity. Let u_0^* and u_1^* be the control inputs given at instants $k = 0$ and $k = 1$ respectively. These inputs can be selected at random.

Initial Data-Collection Period ($k = 1, 2$): Let x_0 be the initial condition at $k = 0$. Since $x_0 \in \mathscr{D}$ and $\mathscr{D}$ is an open subset of $\mathbb{R}^p$, there exists a sampling time T_1 and small enough control inputs u_0^*, u_1^* such that the trajectories of (3)-(4) remain in $\mathscr{D}$.

Trajectories Beyond $k = 2$**:** The control law (11) can be implemented, and thus substituting (11) in (3), we have:

$$x_i(k+1) = x_i(k) + T(\sigma_i(k) - \hat{\sigma}_i(k) + g_i(\hat{x}(k))) + O_x(T^2) \tag{12}$$

Since $\hat{x}_i(k) - x_i(k) = O_x(T^2)$ and $\hat{\sigma}(k) - \sigma(k) = O_x(T)$, and the from assumption that $g_i(x + O_x(T)) = g_i(x) + O_x(T)$, we obtain

$$x_i(k+1) = x_i(k) + T g_i(x(k)) + O_x(T^2) \tag{13}$$

whose trajectories starting in $\mathscr{D}$, asymptotically (exponentially) converge to the equilibrium x^* (from Assumption (1)). Next, we show the existence of the sampling time T^*, for asymptotic and exponential stability.

Case 1: (Asymptotic stability) Using the converse Lyapunov theorem for asymptotic stability (Theorem 4.17, [20]), there exists a positive definite $V(x)$ and a continuous positive definite $W(x)$ which is bounded on any compact subset of $\mathscr{D}$, such that

$$\begin{aligned} V(x(k+1)) - V(x(k)) &\leq -TW(x(k)) + O_{x^2}(T^2) \\ &\leq -TW(x(k)) + W(x(k))O_{x^2}(T^2) \\ &= TW(x(k))(-1 + T||x(k)||^2) \\ &\leq TW(x(k))(-1 + Tr^2) \end{aligned}$$

where the second inequality comes from the fact that $W(x)O_{x^2}(T^2) = O_{x^2}(T^2)$, whenever $||W(x)|| \leq r$ on $\mathscr{D}$. The last inequality is a consequence of $W(x)$ being bounded on a compact subset of $\mathscr{D}$. By choosing $T \in (0, T^*]$, where $T^* = \min\{T_1, \frac{1}{r^2}\}$, we can guarantee the asymptotic stability of x^*. This concludes the proof.

Case 2: (Exponential Stability) Using the converse Lyapunov theorem(Theorem 4.14, [20]) for an exponentially stable equilibrium point, there exists a positive definite $V(x)$ and $K > 0$, such that

$$\begin{aligned} V(x(k+1)) - V(x(k)) &\leq -TK||x(k)||^2 + O_{x^2}(T^2) \\ &\leq -TK||x(k)||^2 + M_1T^2||x(k)||^2 \\ &= T||x(k)||^2(-K + M_1T) \end{aligned}$$

and $T \in (0, T_2]$, such that $T_2 \leq K/M_1$. Hence choose $T^* = \min\{T_1, T_2\}$ such that the states x_i, $i \in \mathscr{P}$ exponentially converge to x^*. This concludes the proof. □

VI. Discussions

Obviating Persistency of Excitation: Owing to the online nature of the data-driven controller, we do not require the data to be persistently exciting. This is because the data-driven estimator does not involve computing the pseudo-inverses of the matrices Y_i or U_i, which are otherwise needed in offline data-driven control techniques like in [19].

Node-Dynamics with Higher Relative Degree: The control scheme proposed can be generalized to node dynamics with arbitrary relative degree ρ. In this case, the data-driven estimator will require at least $\rho+1$ past samples to reconstruct the present states and extended states.

Sampling Time, Number of Samples and Noise: It can be shown that for an essentially bounded noise in the measurements, the estimation error is at most of order $\sigma_i - \hat{\sigma}_i = O_x(T) + O_{\bar{d}}(T^{-\rho})$ where ρ is the relative degree of the node dynamics and $\bar{d} = \operatorname{ess\,sup}_{t\in\mathbb{R}^+} ||d(t)||$ where $d(t)$ is the additive noise in the sensor measurements. Hence the lower bound on the sampling time is dictated by the amount of noise in the system. The effect of noise can also be reduced by increasing the number of samples collected for estimation. This is because the estimator averages out the noise over a larger sample size.

VII. Simulations

In this section, we validate the results presented in Section V using simulations. To this end, we use a network of Kuramoto oscillators that model a large variety of systems like the power grid, synchronized behavior of neurons in the brain, etc. We show how online data-driven control can be implemented to control the states in Kuramoto oscillators and achieve behaviors like synchronization, traveling waves, and clustering when the underlying graph topology is unknown. Consider the Kuramoto dynamics (14) on a graph $\mathscr{G} = (\mathscr{V}, \mathscr{E})$ with $n = 10$ nodes and an edge set $\mathscr{E}$ with control injections u_i.

$$\dot{\theta}_i(t) = \omega_i + \sum_{j=1}^{10} a_{ij}\sin(\theta_j - \theta_i) + b_i u_i,\ y_i = c_i\theta_i \qquad (14)$$

where y_i is the output of the i^{th} node. Note that the (unknown)adjacency matrix need not be symmetric, i.e. the graph can be undirected. Let the underlying topology be as shown in Fig 2. The objective here is to modify the behavior of the nodes in subgraph $\mathscr{P} = \{1, 2, \ldots, 5\}$, such that they achieve synchrony, phase balance or form clusters, by injecting appropriate control signals. The rest of the nodes in the system form subgraphs B and C. Note that the subgraph B is a tree and C is a complete graph, both of which have almost global synchronizing behavior (refer [21], [22]), and hence have an equilibrium that is asymptotically stable. This guarantees that the system is minimum-phase. We also assume that the oscillators are homogenous, i.e. $\omega_i = \omega_j = \omega\ \forall i, j \in \mathscr{V}$. We set $\omega = 1\ rad/s$ for the simulations. The response of the system without the control input, (i.e. setting $u_i = 0\,\forall i \in \mathscr{P}$ and initial conditions $\theta_0 = \{\frac{\pi}{5}, 0.9 + 2\frac{\pi}{5}, 4\frac{\pi}{5}, 0.1 + 8\frac{\pi}{5}, -0.1 + 8\frac{\pi}{5}, 4\frac{\pi}{5}, 4\frac{\pi}{5}, 0, 0, 0\}$). The state trajectories are given in Fig 3. Note that the states θ_i are plotted in the synchronous (rotating) frame of reference, i.e. with a change of coordinates $\theta_i(t) \to \theta_i(t) - \omega_s t$ where ω_s is the mean of all ω_i. Next, we design the coupling function $g_i(\cdot)$ for the required behavior (synchronizing, Phase Balancing, and Cluster Formation). The sampling time is chosen to be $T = 0.05$s.

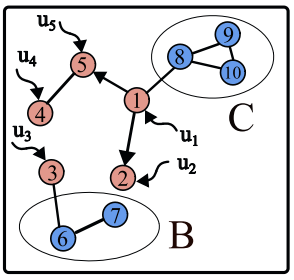

Fig. 2. The Underlying topology of the network: The set of nodes $\mathscr{P}$ are shown in red, with their corresponding input injections. The subgraph B with nodes {6, 7} is connected to node 3 and forms a tree. The subgraph B with nodes {8, 9, 10} are connected to node 1 and form a complete graph.

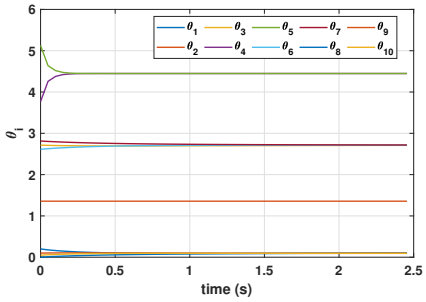

Fig. 3. When control inputs are zero: The states converge to some equilibrium point in the synchronous frame.

1) Case 1 (**Synchronization**): For synchronization, we design the coupling such that nodes form a complete graph (Refer Fig 5.a), as it supports an almost global exponentially stable synchronizing equilibrium point [23]. (Note that several other topologies such as trees will also exhibit almost global synchronization). We do not change the oscillator frequencies and assume $\omega_i = 1$ rad/s $\forall\ i \in \mathscr{P}$. The desired adjacency matrix $A_p^{\text{des}} \in \mathbb{R}^{5\times 5}$ for the subgraph $\mathscr{P}$ and the corresponding coupling functions are

$$A_p^{\text{des}} = \begin{bmatrix} 0 & 1 & 1 & 1 & 1 \\ 1 & 0 & 1 & 1 & 1 \\ 1 & 1 & 0 & 1 & 1 \\ 1 & 1 & 1 & 0 & 1 \\ 1 & 1 & 1 & 1 & 0 \end{bmatrix}$$

$$g_i(\theta) = 1 + \sum_{i=1,\, i\neq j}^{5} \sin(\theta_j - \theta_i). \qquad (15)$$

States vs time plots given in Fig 4 depict how the states converge to the same value (consensus) exponentially.

2) Case 2: (**Phase Balancing**) Phase balancing of oscillators is achieved when the states are equally spaced on the unit circle, i.e. $\mathscr{M} = \{\theta \in \mathbb{T}^p : |\sum_{j=1}^{p} e^{i\theta_j}/n| = 0\}$ (Refer [24]). In order to achieve phase balancing, the topology has to be designed in such a way that the stable equilibrium point belongs to the set $\mathscr{M}$. For a homogenous Kuramoto oscillator on a 5-node graph, a cyclic graph (Refer Fig 5.b) has a stable phase

balancing equilibrium point [25]. Hence the desired adjacency matrix for the nodes in $\mathscr{P}$ is

$$A_p^{\text{des}} = \begin{bmatrix} 0 & 1 & 0 & 0 & 1 \\ 1 & 0 & 1 & 0 & 0 \\ 0 & 1 & 0 & 1 & 0 \\ 0 & 0 & 1 & 0 & 1 \\ 1 & 0 & 0 & 1 & 0 \end{bmatrix}.$$

Similar to Case 1, we derive the coupling functions, keeping the desired frequency of oscillation constant. The initial conditions are chosen inside the region of attraction of the phase-balancing equilibrium point. To demonstrate the robustness of the technique in the presence of noise, we add a zero-mean Gaussian noise with a deviation of 0.05 using the randn() function in MATLAB to the sensor measurements. The states vs time plots for this case are given in Fig 6.

3) Case 3 (**Cluster Formation**): A cluster is a group of nodes that are in phase synchrony. In a heterogeneous Kuramoto oscillator, multiple clusters can be formed based on the coupling weights and the frequencies of the oscillators. Specifically, the clusters have been shown to be stable when the intra-cluster couplings are sufficiently stronger than the inter-cluster coupling, the natural frequencies of nodes in a cluster are homogenous and the natural frequencies of the oscillators belonging to different clusters are sufficiently heterogeneous (Refer [26]). Let the nodes $C_1 = \{1, 2, 3\}$ form a cluster and let $C_2 = \{4, 5\}$ form a second cluster which is at a fixed phase difference with respect to C_1. To this end, first, we design the desired adjacency matrix for the subgraph $\mathscr{P}$ such that the inter-cluster couplings are weaker than the intra-cluster couplings. Let the desired adjacency matrix be

$$A_p^{\text{des}} = \begin{bmatrix} 0 & 60 & 60 & 5 & 0 \\ 60 & 0 & 60 & 0 & 0 \\ 60 & 60 & 0 & 0 & 0 \\ 5 & 0 & 0 & 0 & 60 \\ 0 & 0 & 0 & 60 & 0 \end{bmatrix}.$$

The corresponding network is shown in Fig 5.c, where the nodes in C_1 and C_2 are connected as complete subgraphs with coupling strength of 60. Choosing the inter-cluster coupling $a_{\text{inter}} << 60$ and the cluster frequencies $\omega_{c1} = 5$ and $\omega_{c2} = 2$, we get a constant phase difference between the clusters. Varying these three values varies the phase difference between the clusters. Fig 7 shows how the states, of the nodes in subgraph $\mathscr{P}$, evolve and form two clusters oscillating with a constant phase difference between them. Note that these plots are in the static frame and not in the synchronous frame as in Fig 4 and Fig 6.

Remark 3 (Choice of Desired Topologies)**.** *In the case of synchronization, any connected undirected network, can be designed for local exponential stability of the equilibrium point [24]. The choice of a complete graph is made in*

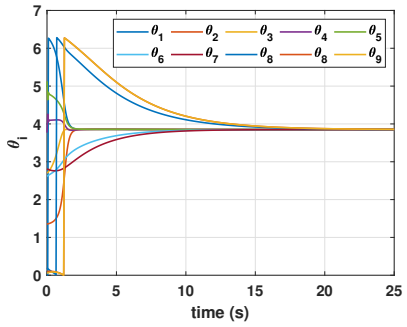

Fig. 4. Case 1: The states corresponding to the nodes in $\mathscr{P}$ converge to span$\{\mathbf{1}_p\}$(consensus), in the synchronous frame, thus oscillating in phase due to the control injected at the nodes. The nodes in $\mathscr{V} \setminus \mathscr{P}$, due to their connected topology, synchronize to the same consensus value.

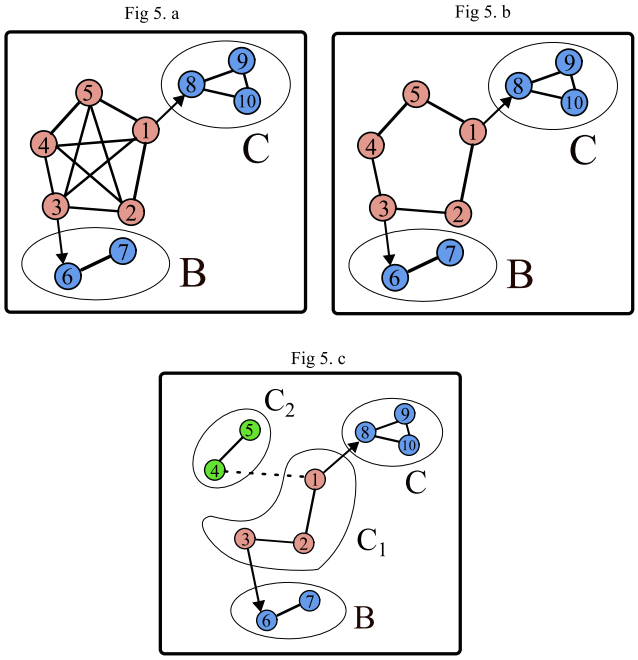

Fig. 5. In Fig 5.a The nodes in $\mathscr{P}$ form a complete graph as the control input eliminates the existing incoming edges and assigns the desired coupling in feedback. In Fig 5.b The nodes in $\mathscr{P}$ form a cycle in feedback, due to the control input and the desired coupling functions. In Fig 5.c Nodes in C_1 (in red) and C_2 (in green) form two clusters, where the dashed line represents the weak inter-cluster coupling and the solid lines represent the strong intra-cluster couplings. The blue nodes belong to $\mathscr{V} \setminus \mathscr{P}$.

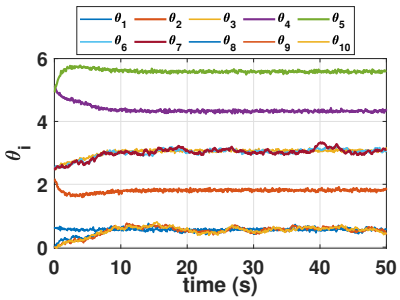

Fig. 6. Case 2: The states converge to a small neighborhood around the phase balancing equilibrium asymptotically, in the synchronous frame in the presence of noise. Similar to case 1, the states $\{\theta_6, \theta_7\}$ converge to θ_3 and $\{\theta_8, \theta_9, \theta_{10}\}$ converge to θ_1.

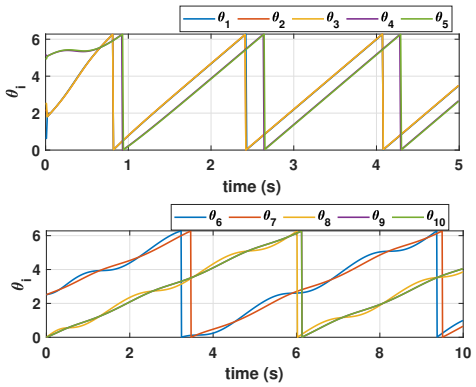

Fig. 7. Case 3: The states $\{\theta_1, \ldots, \theta_5\}$ form two clusters, and oscillate with a constant phase difference between the clusters (in the static frame). The states $\{\theta_6, \ldots, \theta_{10}\}$ also converge to an oscillatory behavior.

order to utilize its almost global synchronization property, which provides us with the largest region of attraction, with the highest convergence rate. As for Case 2, the only 5-node network that has a locally stable phase balancing equilibrium is a cycle graph. In Case 3, we can design the edge weights and the oscillator frequencies such that any set of nodes can be made to form clusters. In all three cases, we can adjust the edge weights to alter the convergence rates.

VIII. CONCLUSIONS

The article discusses the online data-driven control of nonlinear network systems with unknown edges. The control technique introduced provides a method to assign a desired topology to the network when the underlying topology is unknown. The proposed results guarantee the existence of a sampling time such that the network states flow along a desired vector field locally, and converge to the desired equilibrium point. Unlike the state-of-the-art offline data-driven techniques, the control law does not require any persistently exciting data. The method also reduces the number of data points used for estimating the state and the value of the nonlinear coupling between the agents at each instant. We provide simulations-based validation of the results proposed using Kuramoto oscillators and show that behaviors like synchronization, phase balancing, and cluster synchronization can be achieved even in the presence of essentially bounded measurement noise by assigning the required network topology. Network systems like the human brain or communication networks, in practice, do not have a static network topology, but rather a network whose interconnections switch from one topology to another. These networks are referred to as temporal networks, and hence, as part of ongoing research, the authors are now focusing on expanding the results to temporal networks.

REFERENCES

[1] J. Buck, "Synchronous rhythmic flashing of fireflies. ii." *The Quarterly Review of Biology*, vol. 63, no. 3, pp. 265–289, 1988, pMID: 3059390.

[2] D. C. Michaels, E. P. Matyas, and J. Jalife, "Dynamic interactions and mutual synchronization of sinoatrial node pacemaker cells. a mathematical model," *Circ Res*, vol. 58, no. 5, pp. 706–720, May 1986.

[3] A. Saradagi, V. Muralidharan, V. Krishnan, S. Menta, and A. D. Mahindrakar, "Formation control and trajectory tracking of non-holonomic mobile robots," *IEEE Transactions on Control Systems Technology*, vol. 26, no. 6, pp. 2250–2258, 2018.

[4] T. Menara, G. Baggio, D. S. Bassett, and F. Pasqualetti, "Stability conditions for cluster synchronization in networks of heterogeneous kuramoto oscillators," *IEEE Transactions on Control of Network Systems*, vol. 7, no. 1, pp. 302–314, 2020.

[5] R. Delabays, S. Jafarpour, and F. Bullo, "Multistability and anomalies in oscillator models of lossy power grids," *Nature Communications*, vol. 13, no. 1, p. 5238, Sep. 2022.

[6] F. Pasqualetti, S. Zampieri, and F. Bullo, "Controllability metrics, limitations and algorithms for complex networks," *IEEE Transactions on Control of Network Systems*, vol. 1, no. 1, pp. 40–52, 2014.

[7] M. V. Srighakollapu, R. K. Kalaimani, and R. Pasumarthy, "Optimizing driver nodes for structural controllability of temporal networks," *IEEE Transactions on Control of Network Systems*, vol. 9, no. 1, pp. 380–389, 2022.

[8] Y. Tian, P. Jia, A. MirTabatabaei, L. Wang, N. E. Friedkin, and F. Bullo, "Social power evolution in influence networks with stubborn individuals," *IEEE Transactions on Automatic Control*, vol. 67, no. 2, pp. 574–588, 2022.

[9] G. Deco, M. L. Kringelbach, V. K. Jirsa, and P. Ritter, "The dynamics of resting fluctuations in the brain: metastability and its dynamical cortical core," *Scientific Reports*, vol. 7, no. 1, p. 3095, Jun. 2017.

[10] J.-S. Brittain and H. Cagnan, "Recent trends in the use of electrical neuromodulation in parkinson's disease," *Curr Behav Neurosci Rep*, vol. 5, no. 2, pp. 170–178, Apr. 2018.

[11] K. Lehnertz, S. Bialonski, M.-T. Horstmann, D. Krug, A. Rothkegel, M. Staniek, and T. Wagner, "Synchronization phenomena in human epileptic brain networks," *J Neurosci Methods*, vol. 183, no. 1, pp. 42–48, May 2009.

[12] S. Chiken and A. Nambu, "Mechanism of deep brain stimulation: Inhibition, excitation, or disruption?" *Neuroscientist*, vol. 22, no. 3, pp. 313–322, Apr. 2015.

[13] T. Menara, G. Baggio, D. S. Bassett, and F. Pasqualetti, "Conditions for feedback linearization of network systems," *IEEE Control Systems Letters*, vol. 4, no. 3, pp. 578–583, 2020.

[14] C. De Persis and P. Tesi, "Formulas for data-driven control: Stabilization, optimality, and robustness," *IEEE Transactions on Automatic Control*, vol. 65, no. 3, pp. 909–924, 2020.

[15] D. Gadginmath, V. Krishnan, and F. Pasqualetti, "Data-driven feedback linearization using the koopman generator," 2022. [Online]. Available: https://arxiv.org/abs/2210.05046

[16] J. G. Rueda-Escobedo, E. Fridman, and J. Schiffer, "Data-driven control for linear discrete-time delay systems," *IEEE Transactions on Automatic Control*, vol. 67, no. 7, pp. 3321–3336, 2022.

[17] L. Fraile, M. Marchi, and P. Tabuada, "Data-driven stabilization of siso feedback linearizable systems," *arXiv:2003.14240*, 2020.

[18] K. Shenoy, A. Saradagi, R. Pasumarthy, and V. Chellaboina, "Data-driven feedback linearization of nonlinear systems with periodic orbits in the zero-dynamics," 2022.

[19] G. Baggio, D. S. Bassett, and F. Pasqualetti, "Data-driven control of complex networks," *Nature Communications*, vol. 12, no. 1, p. 1429, Mar. 2021.

[20] H. Khalil, *Nonlinear Systems*, ser. Pearson Education. Prentice Hall, 2002.

[21] F. Dörfler and F. Bullo, "Synchronization in complex networks of phase oscillators: A survey," *Automatica*, vol. 50, pp. 1539–1564, 2014.

[22] A. H. Dekker and R. Taylor, "Synchronization properties of trees in the kuramoto model," *SIAM Journal on Applied Dynamical Systems*, vol. 12, no. 2, pp. 596–617, 2013.

[23] E. Canale and P. Monzon, "Almost global synchronization of symmetric kuramoto coupled oscillators," in *Systems Structure and Control*, P. Husek, Ed. Rijeka: IntechOpen, 2008, ch. 8.

[24] F. Bullo, *Lectures on network systems*. Kindle Direct Publishing, 2020, vol. 1.

[25] A. Townsend, M. Stillman, and S. H. Strogatz, "Dense networks that do not synchronize and sparse ones that do," *Chaos: An Interdisciplinary Journal of Nonlinear Science*, vol. 30, no. 8, p. 083142, 2020.

[26] T. Menara, G. Baggio, D. S. Bassett, and F. Pasqualetti, "Stability conditions for cluster synchronization in networks of heterogeneous kuramoto oscillators," *IEEE Transactions on Control of Network Systems*, vol. 7, no. 1, pp. 302–314, 2020.